Mining S-PLUS for Metal-Poor Stars in the Milky Way

12-15

arxiv:2206.09003v1

Reporter: Baokun Sun

Outline

- 1. Introduction
- 2. Target selection and observations
- 3. Stellar parameters and chemical abundances
- 4. Analysis and Discussion
- 5. Conclusions

Introduction

- Very Metal-Poor (VMP - [Fe/H]< -2.0; Beers & Christlieb 2005) stars are the "local" observational probes that allow astronomers to address questions at cosmological scales (Bromm & Larson 2004).

- Ivezi´c et al. (2008) were able to determine temperatures (with typical uncertainties of ~100 K) and metallicities (with uncertainties of 0.2 dex or better for $-2.0 \leq$[Fe/H]≤ -0.5) for over 2 million F/G stars in the Milky Way.

- One of the limitations on the low-metallicity end is due to the broadness of the u filter, which loses its metallicity sensitivity, hampering efforts to extend the determinations to [Fe/H]≤ -2.5.

Introduction

- The Javalambre Photometric Local Universe Survey (J-PLUS; Cenarro et al. 2019) and the Southern Photometric Local Universe Survey (S-PLUS; Mendes de Oliveira et al. 2019) have a unique 12 broad- and narrow band filter set, consisting of four SDSS (g, r, i, z), one modified SDSS u, and seven narrow-band filters.

- The names and key absorption features sampled by the narrow-band filters are: J0378 – [O II]; J0395 – Ca II H+K; J0410 – Hδ; J0430 – G band; J0515 – Mg b triplet; J0660 – Hα; and J0861 – Ca triplet.
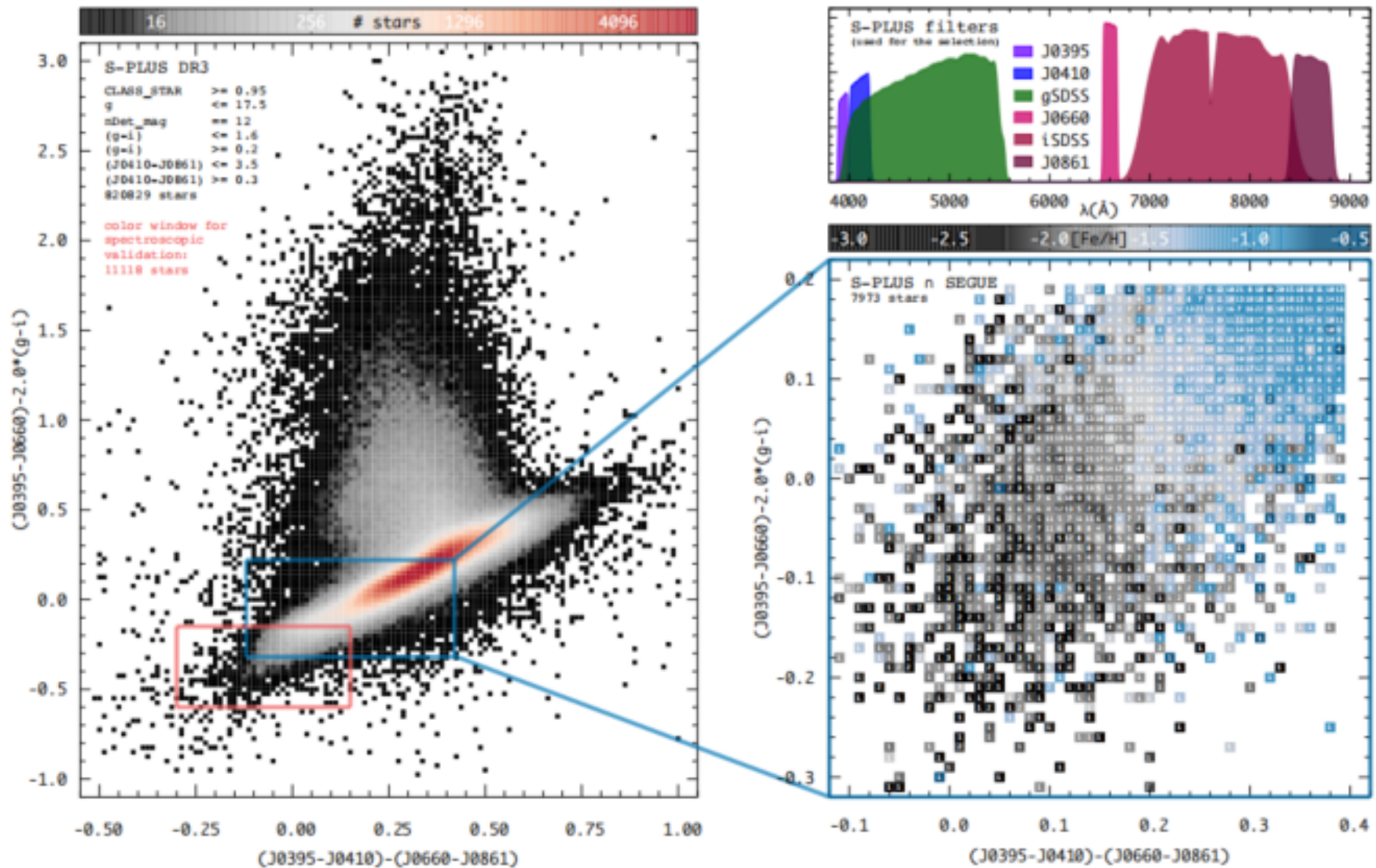
- (ar;
- g
  r
- r.
  r.
- (
  c   d
  c
- (;
-] **Figure 1.** Left panel: stellar density for the selected S-PLUS DR3 sample in a color-color diagram. The red box outlines the color window for the spectroscopic follow-up (see text for details). The inset (bottom right panel) shows the cross-match with the SDSS/SEGUE spectroscopic database, color-coded by the average metallicity in each bin. The number of stars in each bin is also shown. Top right panel: S-PLUS transmission curves for the six narrow-band and broad band filters used in this selection.
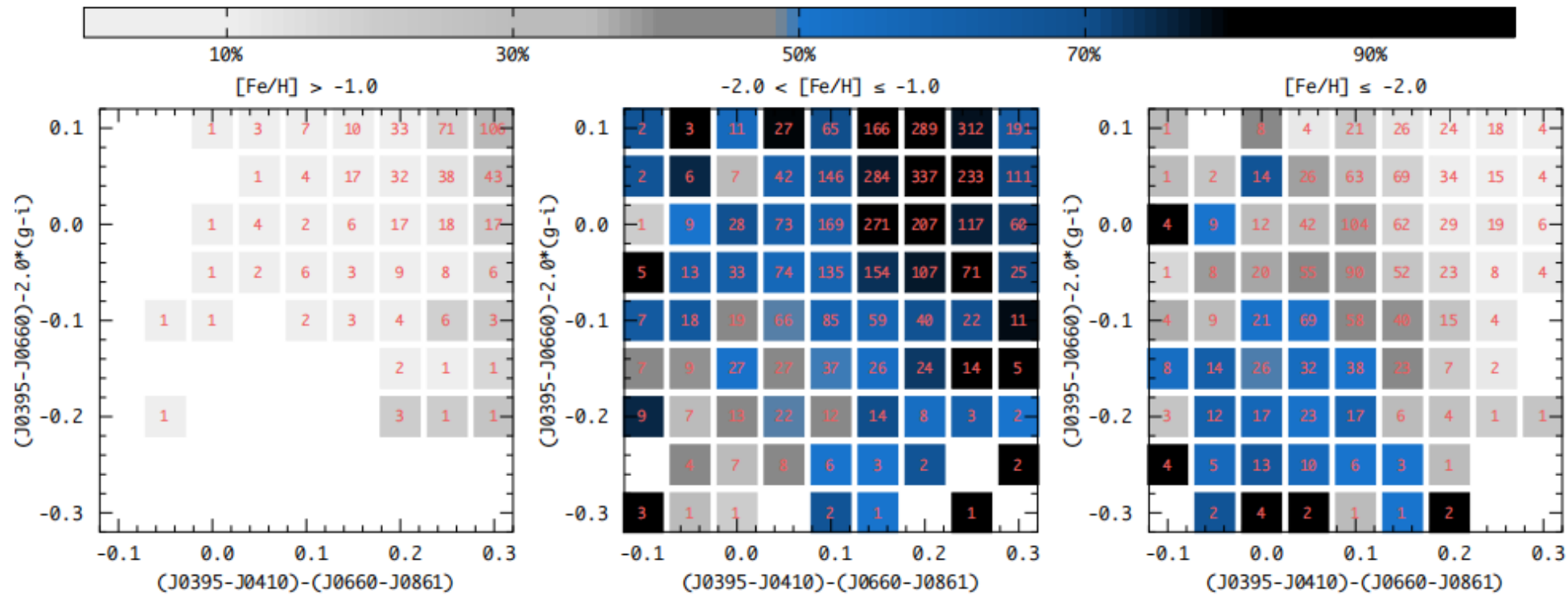
5

Figure 2. Color-color diagram for three different [Fe/H] regimes. The bins in each panel are color-coded by the fraction of stars with an average metallicity in a given range. The number of stars in each bin is also shown.

For the spectroscopic follow-up, from the right panel, a cut was made where most bins have at least a 50% fraction of [Fe/H]≤ -2.0 star. Within this window, which contains 11,118 stars from S-PLUS DR3.

Medium-Resolution Spectroscopy

- CTIO Blanco Telescope —A total of 384 stars were observed with the V́ıctor M. Blanco 4-meter Telescope. The exposure times ranged from 90 to 1800 seconds, with a total of 57.96 hours on target.

- Gemini South Telescope —138 stars were observed with the 8.1 m Gemini South telescope and the GMOS. The exposure times ranged from 210 to 1800 seconds, with a total of 45.84 hours on target.

Stellar parameters and chemical abundances

- The determinations of stellar atmospheric parameters (Teff, log g, and [Fe/H]), carbonicity ([C/Fe]), and α-to iron ratios ([α/Fe]) for the stars observed as part of spectroscopic follow-up were made using the n-SSPP.

- The code uses photometric and spectroscopic information to calculate the atmospheric parameters based on several different methods, including calibrations with spectral line indices (from the Ca II H and K lines for [Fe/H]), photometric Teff predictions, and synthetic spectra matching.

- The [C/Fe] and [α/Fe] are estimated from the strength of the CH G-band molecular feature at ~ 4300 ˚A and the Mg I triplet at 5150–5200 ˚A, respectively.

[Fe/H] sensitivity from narrow-band photometry

For the SEDs on the top set, all Teff values are within 18 K, which translates into a 0.09 mag (~ 0.5%) variation in the J0660 flux. As expected, there is an increase of the J0395 magnitude with [Fe/H]. The two extremes of the [Fe/H] scale have a 0.36 magnitude difference in J0395, which roughly translates into a 2.0 dex variation in [Fe/H].
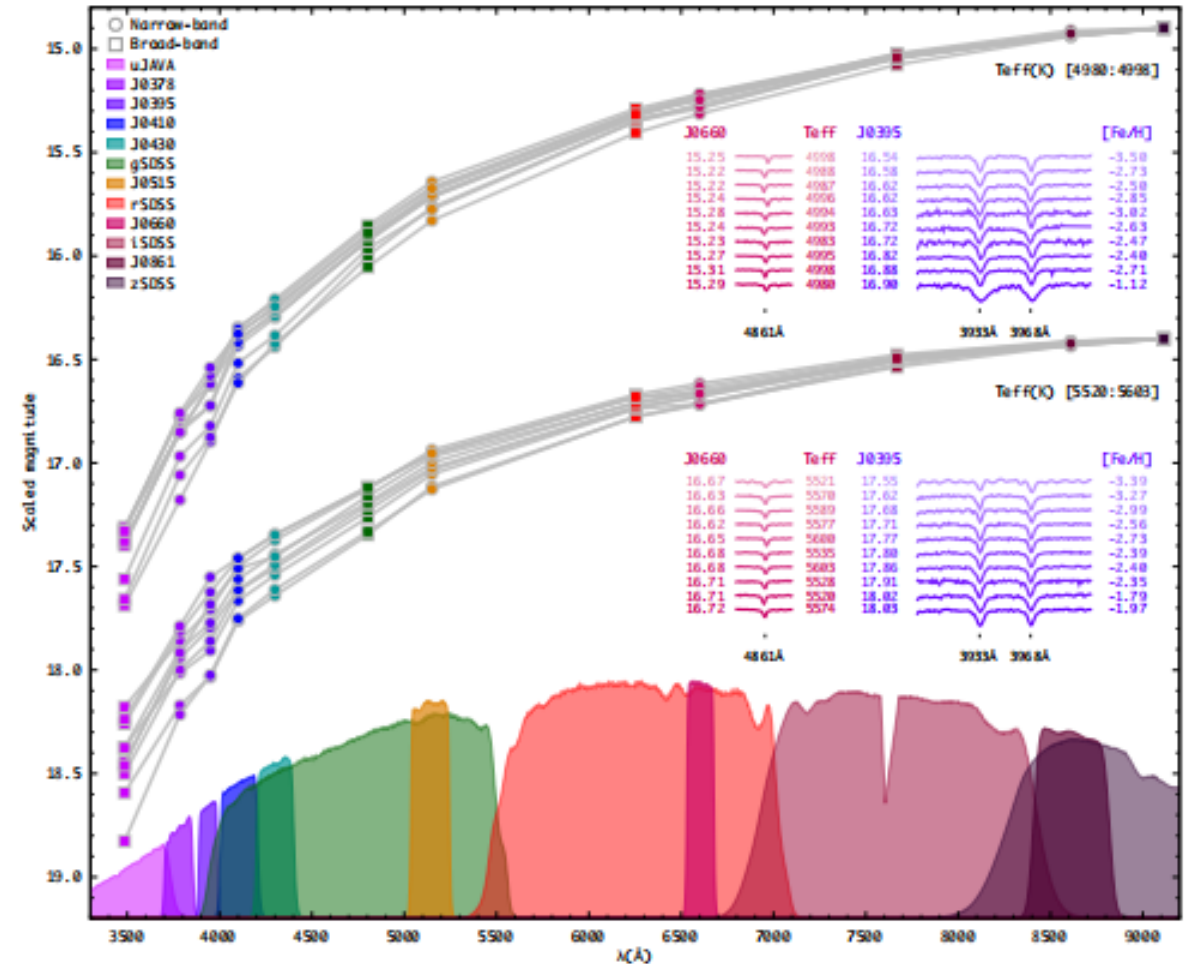

Figure 6. Spectral energy distribution (SED) for 20 selected program stars from Blanco and Gemini. Magnitudes were scaled to zSDSS=14.9 (top) and 16.4 (bottom). The temperature range for each set is displayed right below the SEDs. The insets show the observed spectra around the Hβ and Ca II HK absorption features, sorted by their J0395 scaled magnitude. Also shown are the T_{eff} and [Fe/H] for each star and the S-PLUS transmission curves. See text for further details.

[Fe/H] sensitivity from narrow-band photometry

To a certain degree, the same applies to the bottom set of SEDs, which has an average Teff about 500 K warmer than the top set. For this group, the variation in the J0660 magnitude is very small (0.05 mag), while the difference between the extremes in J0395 (0.48 mag) still translates into a 1.5 dex range in terms of [Fe/H].
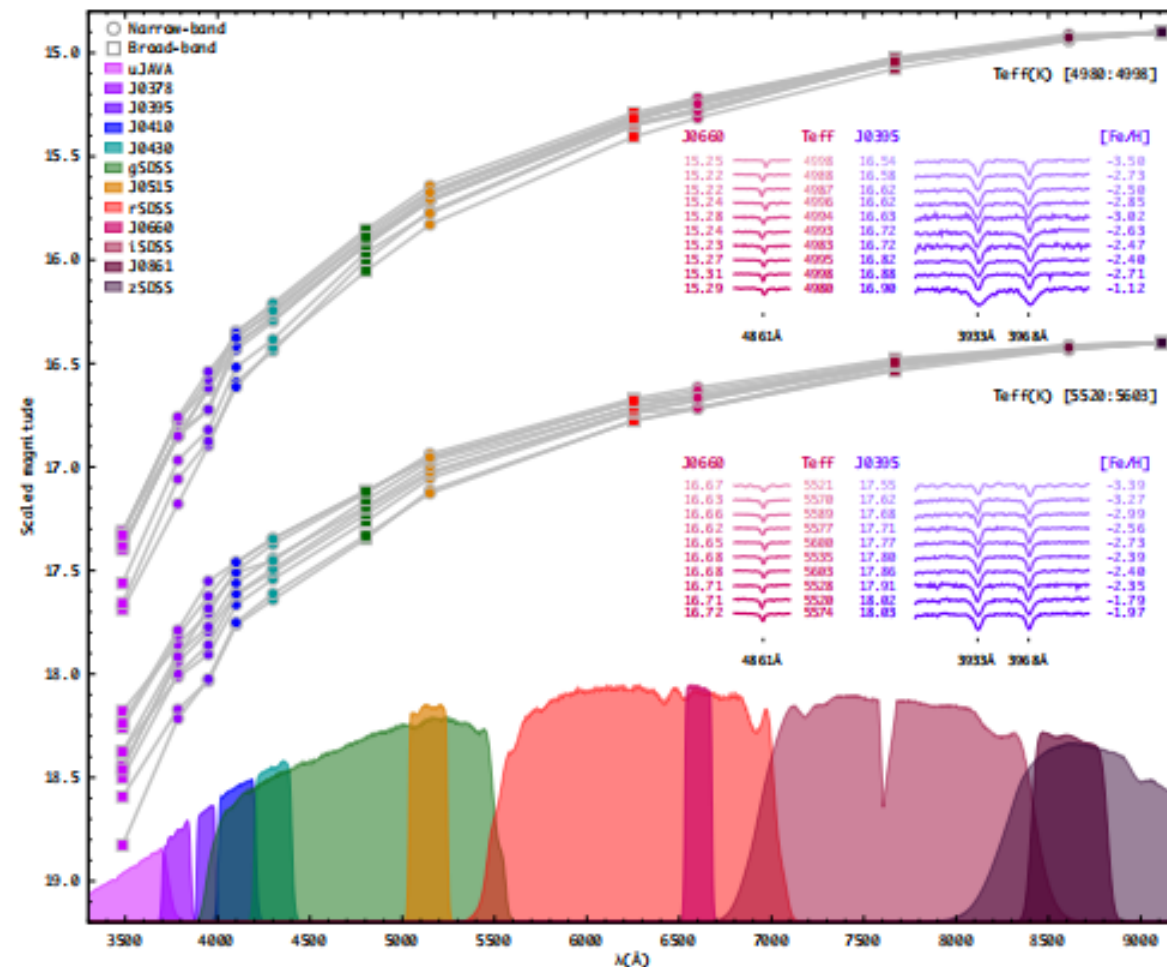

Figure 6. Spectral energy distribution (SED) for 20 selected program stars from Blanco and Gemini. Magnitudes were scaled to zSDSS=14.9 (top) and 16.4 (bottom). The temperature range for each set is displayed right below the SEDs. The insets show the observed spectra around the Hβ and Ca II HK absorption features, sorted by their J0395 scaled magnitude. Also shown are the T_{eff} and [Fe/H] for each star and the S-PLUS transmission curves. See text for further details.

The success rate for [Fe/H]≤ −2.0 is 83% as compared to 60% in Placco et al. (2018), 39% in Placco et al. (2019), and 30% in Limberg et al. (2021b). Finally, the fraction of stars with [Fe/H]≤ −3.0 (15%) is higher than the fraction of stars with [Fe/H]> −1.5 (11%), which confirms the effectiveness of the S-PLUS color window in selecting low-metallicity stars.
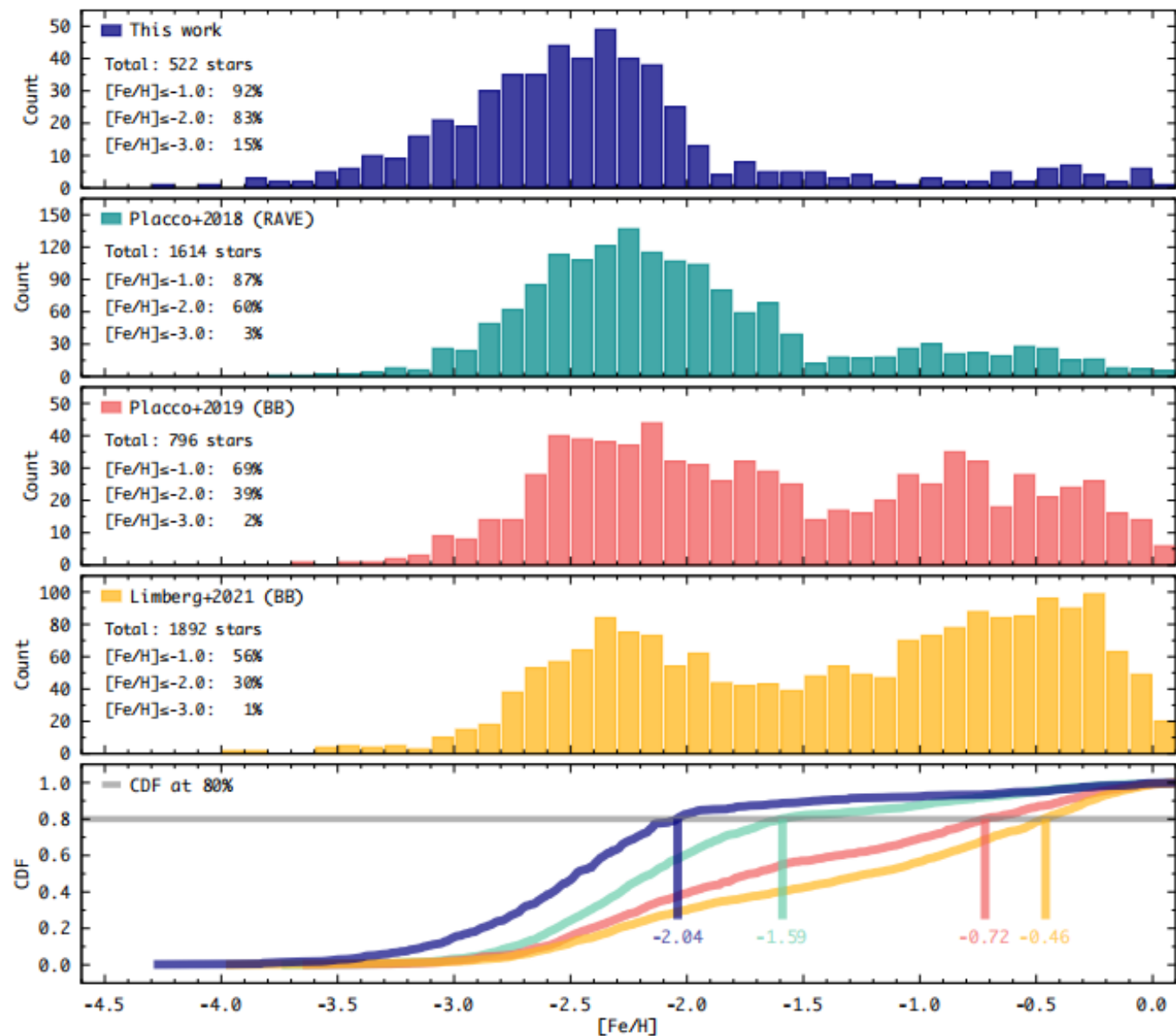

Figure 8. Metallicity histogram for the program stars (top panel), compared with the distributions from Placco et al. (2018), Placco et al. (2019), and Limberg et al. (2021b) (middle panels). Each panel shows the total number of stars and the fractions for different metalliticy regimes. The bottom panel shows the cumulative distribution functions (CDF) for the three samples, marking the [Fe/H] value for which they reach 80%.
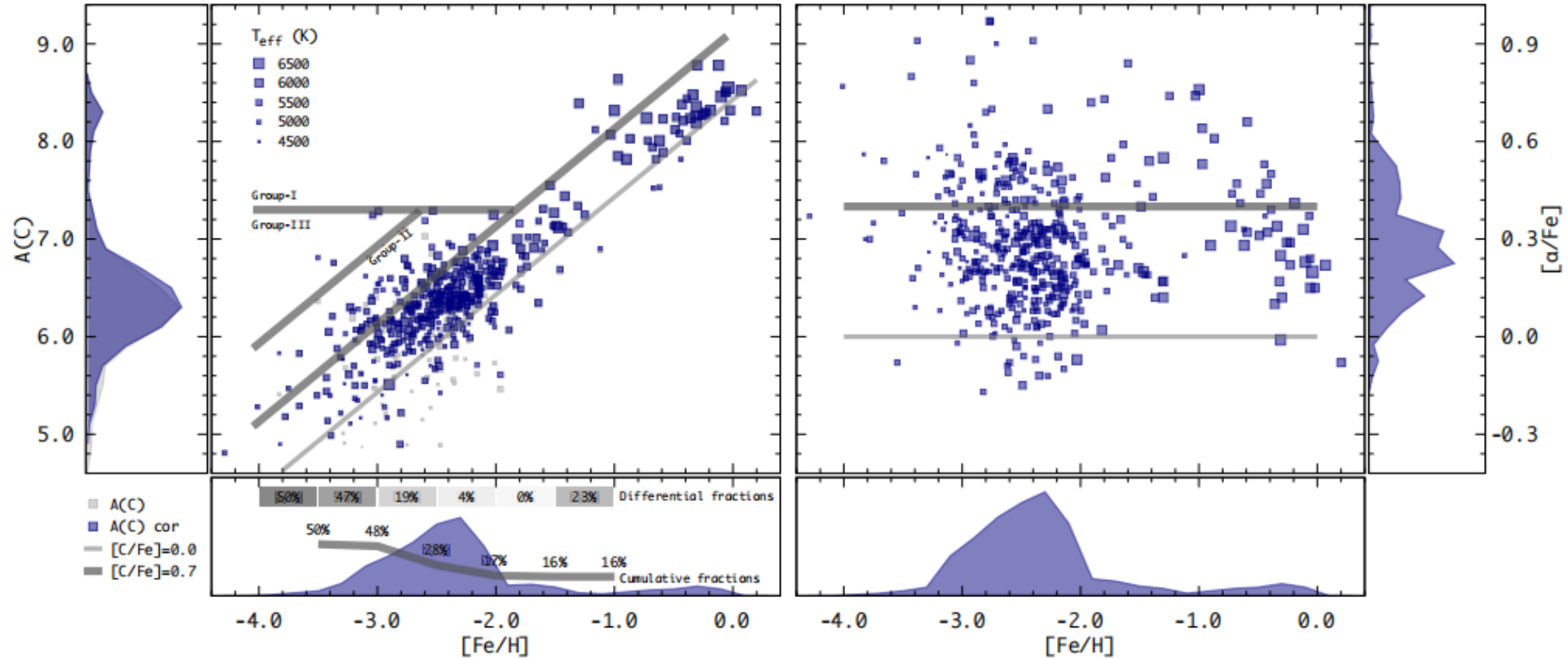
Carbon and α-element abundances

Figure 9. Absolute carbon, (A(C), corrected as described in the text - left panel), and α-element abundance ratios, [α/Fe] (right panel), as a function of the metallicity calculated by the n-SSPP. The side and lower panels show the marginal distributions. The solid line in the lower left panel shows the cumulative CEMP fractions for the stars with $-3.5 \leq$ [Fe/H] ≤ -1.0 and the numbers of the top part of the panel are the differential fractions for 0.5 dex [Fe/H] bins. Point sizes are proportional to $T_{\rm eff}$.

Further inspection of Figure 4 reveals that 42% of the stars with Teff≥ 5900 K have [Fe/H]≥ −1.0, while only 3% of the stars with Teff< 5900 K have [Fe/H]≥ −1.0.

One such candidate is (J0378-i)-(J0410-J0660), which contains the metallicity-sensitive J0378 filter and the temperature-sensitive (J0410-J0660) color index.

For the low color index subsample (blue points), the fractions are 98% for stars with [Fe/H]≤ −1.0 and 88% with [Fe/H]≤ −2.0.
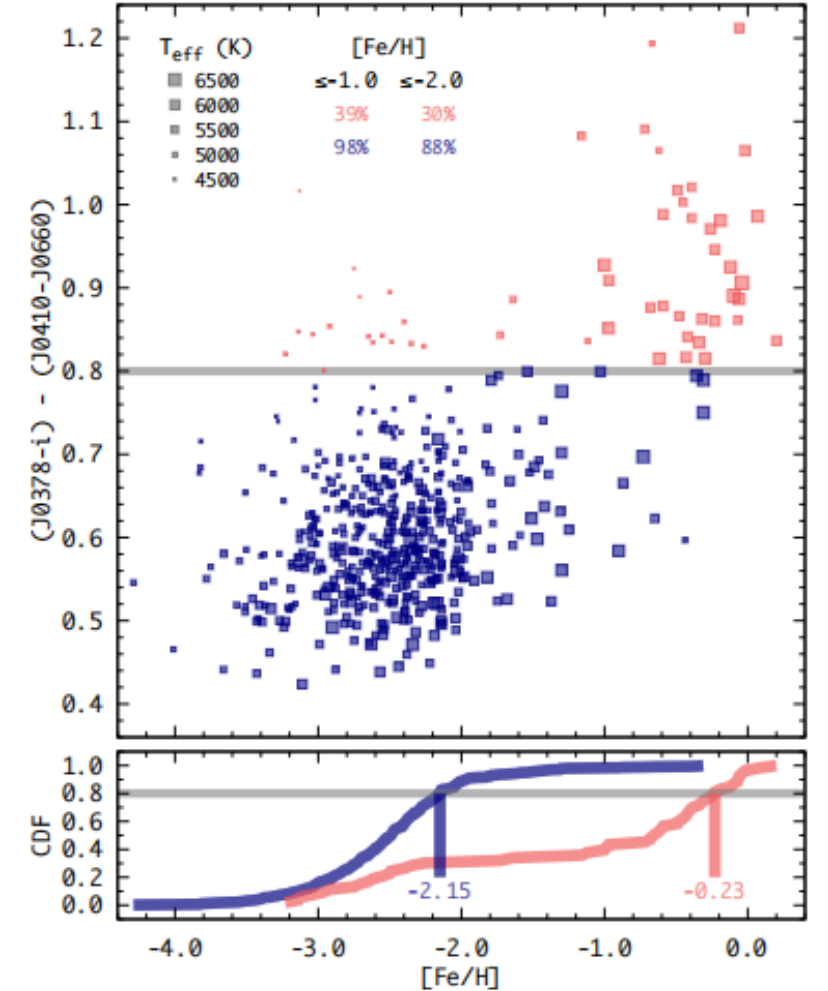

Figure 10. Top panel: (J0378-i)-(J0410-J0660) as a function of the metallicity for the observed sample, with the gray line marking the proposed color cut. Also shown are the fractions of stars with [Fe/H]≤ −1.0 and ≤ −2.0 for the two subsamples. The point sizes are proportional to T_{eff}. Bottom panel: cumulative distribution functions (CDF) for the two subsamples, marking the [Fe/H] value for which they reach 80%.

13

Summary

- This work presented the medium-resolution spectroscopic follow-up of 522 low-metallicity star candidates selected from their S-PLUS photometry.

- By using metallicity-sensitive colors, the success rate found is 92% for [Fe/H]≤ -1.0, 83% for [Fe/H]≤ -2.0, and 15% for [Fe/H]≤ -3.0, including two ultra metal-poor stars ([Fe/H]≤ -4.0).

- Based on the carbonicity determinations, there are 68 CEMP stars in the sample, including 60 Group-II and 4 Group-III.

- Based on the [Fe/H] determined in this work, a further color restriction is proposed, which can potentially increase the fractions of stars with [Fe/H]≤ -1.0 and ≤ -2.0 to 98% and 88%, respectively.